COMPARISON OF METALLOGRAPHY AND MECHANICAL PROPERTIES OF SAMPLES PRINTED FROM WC-CO POWDER MIX USING SLM TECHNOLOGY IN PROTECTIVE ATMOSPHERES OF ARGON AND NITROGEN

David Bricín*, Antonín Kříž

Department of Material Science and Technology, University of West Bohemia in Pilsen, Czech Republic

Abstract

The aim of this study was to compare the properties of samples made from WC-Co powder mixture, printed in two different protective atmospheres, namely nitrogen and argon. An optical and a scanning electron microscope which enables elemental analysis by EDX were used to evaluate the properties of the printed samples. This was further supplemented by analysis of phase composition using X-ray diffraction and of mechanical properties, namely a compression strength test and the Vickers hardness test. Based on a comparison of the results, it was possible to state that the mechanical properties and structure of the samples printed in the protective atmosphere of nitrogen do not differ significantly from the samples printed in the protective atmosphere of argon. Most of the pores that occurred in the structure of the samples were related to the residual moisture of the powder mixture and its other properties. Analysis of the phase composition by X-ray diffraction showed no interaction of nitrogen with the sintered material. Further follow up experiments will search for a suitable WC-Co powder mix for SLM technology. The studies will deal with treatments and processing of the powder mix to create a homogeneous body with minimal internal porosity.

Keywords: *Protective atmosphere, argon atmosphere, nitrogen atmosphere, SLM technology, WC-Co, porosity*

1. INTRODUCTION

Additive technology is currently very important in all fields of industry. *(Venuvinod and Ma, 2010; Pacurar and Pacurar, 2016*) At present, the main focus is on the processing and research of metal and polymer materials using this technology. A slightly neglected area is the processing of carbide powder mixtures. This study deals with processing a commercially available powder-based carbide blend of WC-Co with 30% binder. The particles of this powder mixture are not held together by the binder, but only by the action of adhesive forces, see Figure 1, forming spherical structures of different sizes, as shown Figure 2. The average grain size of this mixture is around 6 μm, but it also contains finer grains smaller than 1 μm.

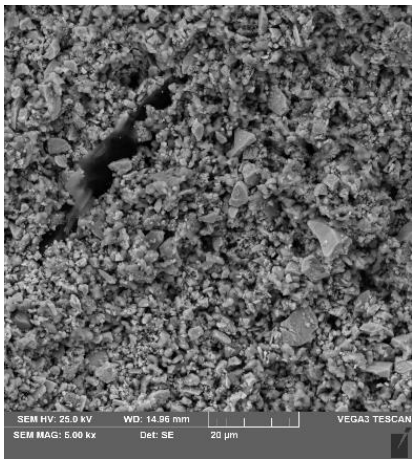


Fig. 1 Powder particles. Average size of the particles is about 6 microns.

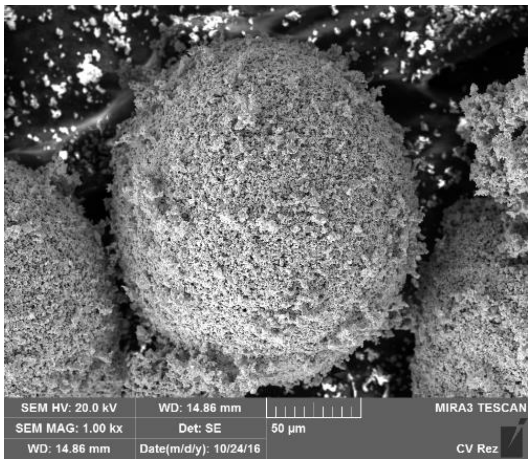


Fig. 2 Globular structures formed by powder particles due to the action of Van der Waals adhesive forces.

This blend was processed under various parameters on an SLM printer. The variable parameters included laser power, scanning speed, and an inert atmosphere of nitrogen or argon, see Table 1. The samples were divided into two groups depending on the protective atmosphere used.

	Inert atmosphere	**Layer thickness (µm)**	**Laser power (W)**	**Scanning speed (mm/s)**
Series of samples A	Argon	100	120-360	100-300
Series of samples B	Nitrogen	100	120-360	100-300

Table 1. Parameters of the experiment

The metallography of the samples was then evaluated using light and scanning electron microscopy. The aim of this evaluation was to map out the occurrence of pores in the structure of the samples, focusing on their shape and size, and analysing their chemical composition using the EDX analyser. An X-ray diffraction analysis was then performed to determine the differences in the phase composition of the samples, and then the mechanical properties tests, namely the Vickers hardness test and the compression strength test.

2. RESULTS AND DISCUSSION

2.1. Metallographic analysis of the samples

Metallographic analysis of the samples was performed using the ZEISS OBSERVER Z1m light microscope and AxioVision software. The aim of this analysis was to determine the proportion of pores in the structure of the samples, to determine their size and shape. After the sample structure was evoked, the tungsten carbide grain size was measured. In addition to metallographic analysis on a light microscope, the samples were analysed using a PHILPS ESEM electron beam scanning microscope with an EDX analyser to analyse the chemical composition of the samples.

Metallographic analysis of pore size and its volume fraction was performed on the samples which were produced under the same boundary conditions, i.e. the same laser power, scanning speed and layer thickness. Ten metallographic sections were prepared for each test sample, and the distance between the

sections was about 50 microns. From each section, a mosaic of images was created to capture the structure of each sample. The structure was then evaluated by Axio Vision software, see Fig 3.

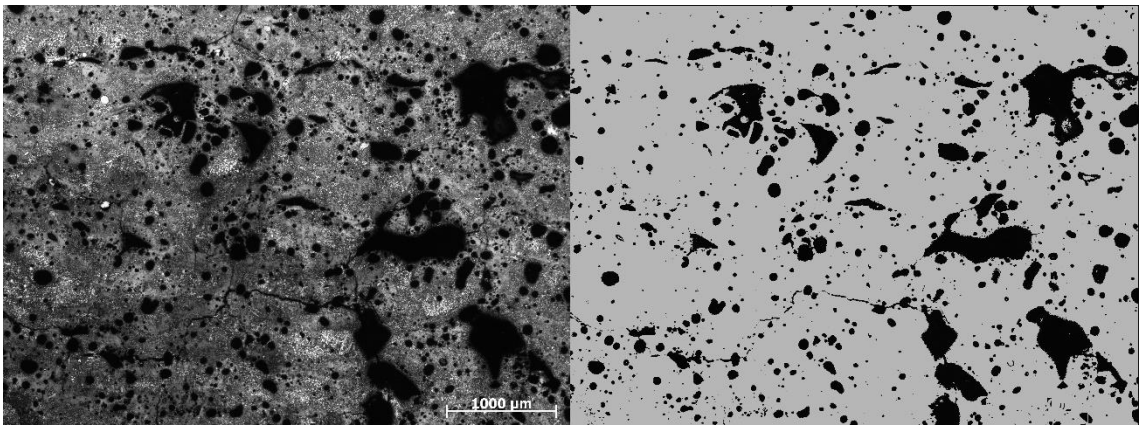


Fig. 3 A mosaic image of the structure of a sample. Left - before binary processing. Right - after binary processing by Axio-Vision software.

From an evaluation of the binary images it was then possible to compile charts that indicate the size of the pores in the structure of the samples, and determine the total porosity or density of the samples depending on the characteristics of their production on the additive manufacturing SLM device, see figs 4-5.

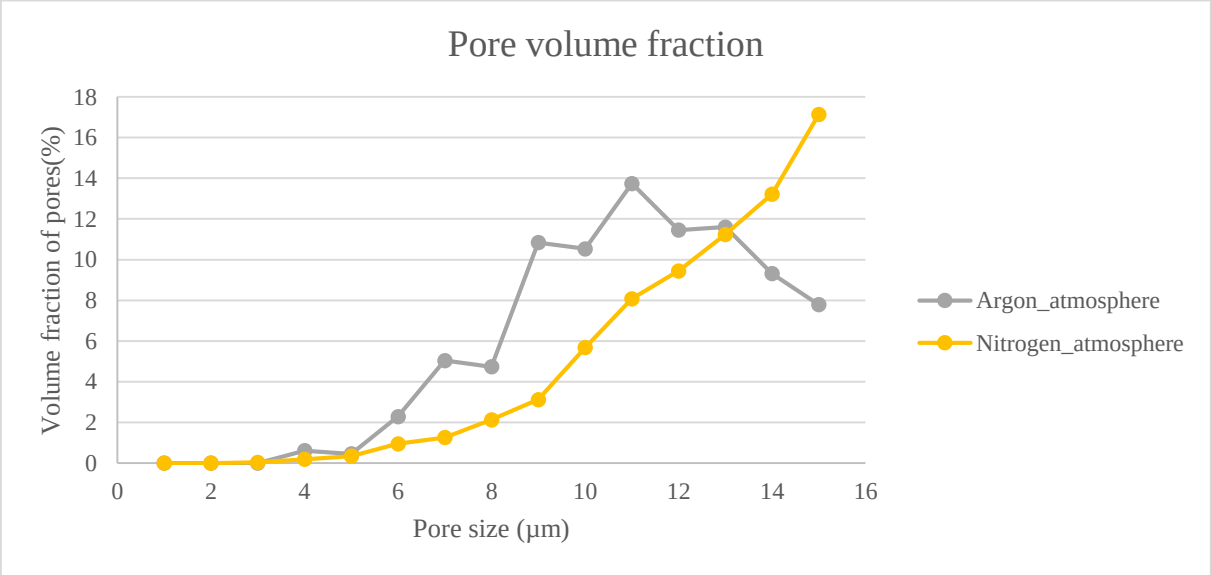


Fig. 4 Volume representation of pore sizes in the structure of samples printed in nitrogen and argon atmospheres

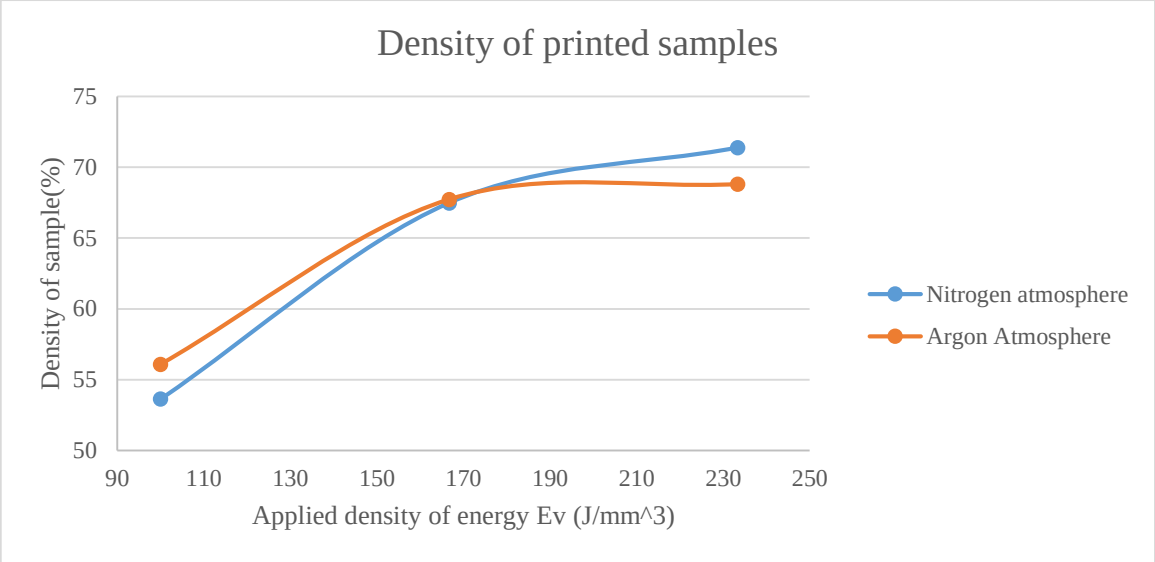


Fig. 5 Density of the printed samples

From the results of the metallographic analysis of the samples before etching, it is possible to say that the pores in the structure of the samples were closed. This was because the input density of the energy was high enough to melt the binder for a sufficient time and therefore it could infiltrate into the free space between the particles of tungsten carbide. The maximum density of the printed samples was about seventy percent in both atmospheres. A higher density of the printed samples was not achieved, probably due to the action of residual moisture and the fact that the powder was not suitable for the SLM Additive Manufacturing Process. *(Sutton et al., 2016)* Residual moisture was confirmed by EDX analysis of the pore surface, which was oxidized. Globular pores, non-globular pores and cracks were observed in each printed sample, see Fig. 3. These defects occurred due to incorrect setting of the boundary conditions of the printing process, the action of residual moisture and thermal stresses. *(Uhlmann, Bergmann and Gridin, 2015; Wang et al., 2002; Bricín, Špirit and Kříž, 2018; GU et al., 2006; Kumar, 2009; Pacurar and Pacurar, 2016; Palán, 2015)* The density and volume distribution of the size of the pores in the samples appears to be almost the same for samples printed in both atmospheres. Differences in the pore size distribution, see Fig. 4, were due to the different size of the discontinuities which were observed in the samples printed in nitrogen and argon atmospheres, see figs. 6-7. These differences may be to the different distribution of the samples on the building plate, which could lead to a different heat distribution in the samples and the building plate, or because the powder which was used was not suitable for the additive manufacturing process. This is because the powder is formed of small particles which create globular structures with a size of more than 100 microns, see Fig. 2, and therefore the powder cannot fall evenly onto the building plate, resulting in a different distribution of sizes and types of pores in the samples which were printed in different atmospheres. It may also be due to the fact that the binder and carbide grains were separate, which could lead to their non-uniform distribution, and this could also be reflected in the porosity of the samples.

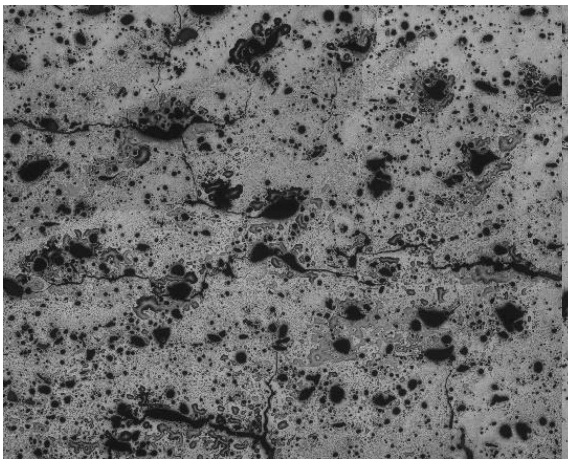


Fig. 6 Structure of pores of sample printed in Argon atmosphere.

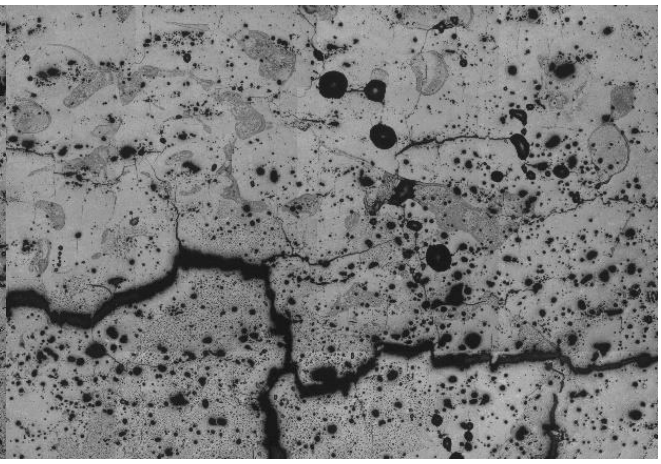


Fig. 7 Structure of pores of sample printed in Nitrogen atmosphere.

After Murakami etching, the WC grains were measured using standard ČSN EN ISO 643 which was then converted to microns, see Table 2. The distribution of the WC grains in the samples was also observed, see figs. 8-9.

Argon Atmosphere	**G11-12**	**6±0.7 (µm)**
Nitrogen Atmosphere	G11-12	6±0.6 (µm)

Table 2. Average size of WC grains

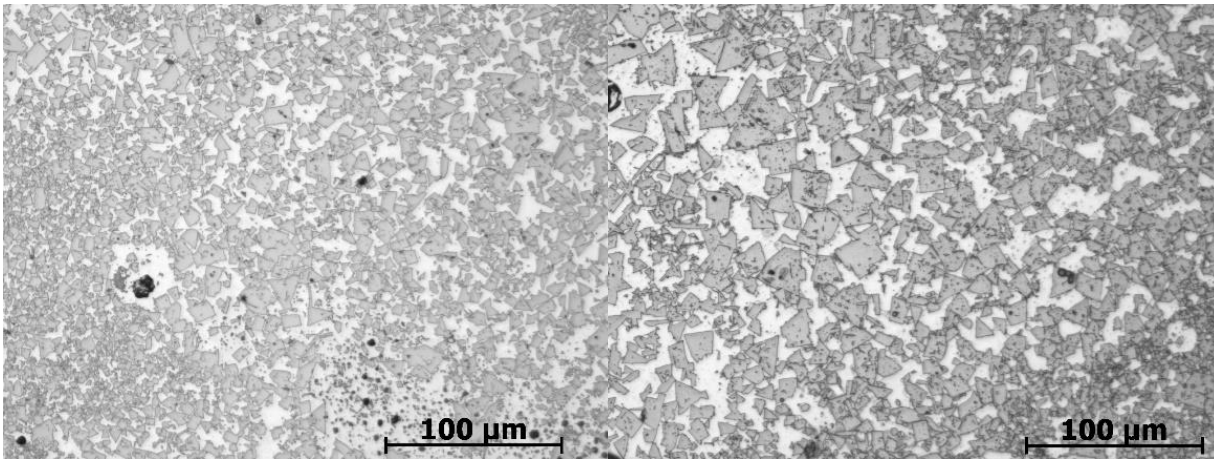


Fig. 8 Distribution of WC grains in sample printed in Argon atmosphere

Fig. 9 Distribution of WC grains in sample printed in Nitrogen atmosphere

The average size of the WC grains corresponds with the average size of the powder particles. The distribution of the grain size of the printed samples was also similar to the powder particle distribution. The distribution of the binder and WC grains was not uniform in the samples printed in both atmospheres. This is because of the type of powder, which consisted of separate grains of binder Co and grains of WC, and also the distribution of the particles was affected by the parameters of the printing process. (*Bricín, Špirit and Kříž, 2018)* It was observed that if a higher scanning speed and laser power was used, the distribution of the WC grains and binder appeared uniform. (*Bricín, Špirit and Kříž, 2018)*

2.2. Mechanical properties and X-ray analysis

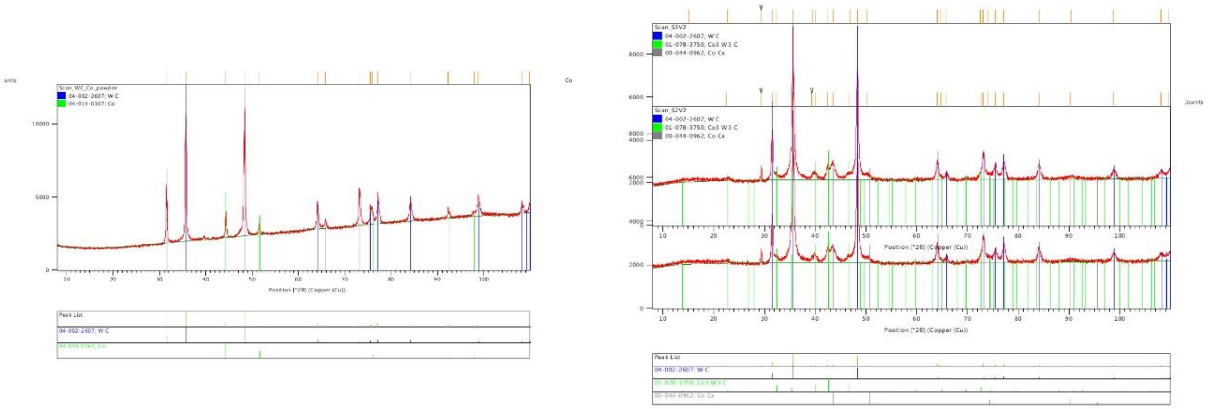


Fig. 10 Results of X-ray phase analysis. Left - powder phase analysis. Right - results of phase analysis of sample printed in Nitrogen atmosphere. Right - result of phase analysis of sample printed in Argon atmosphere.

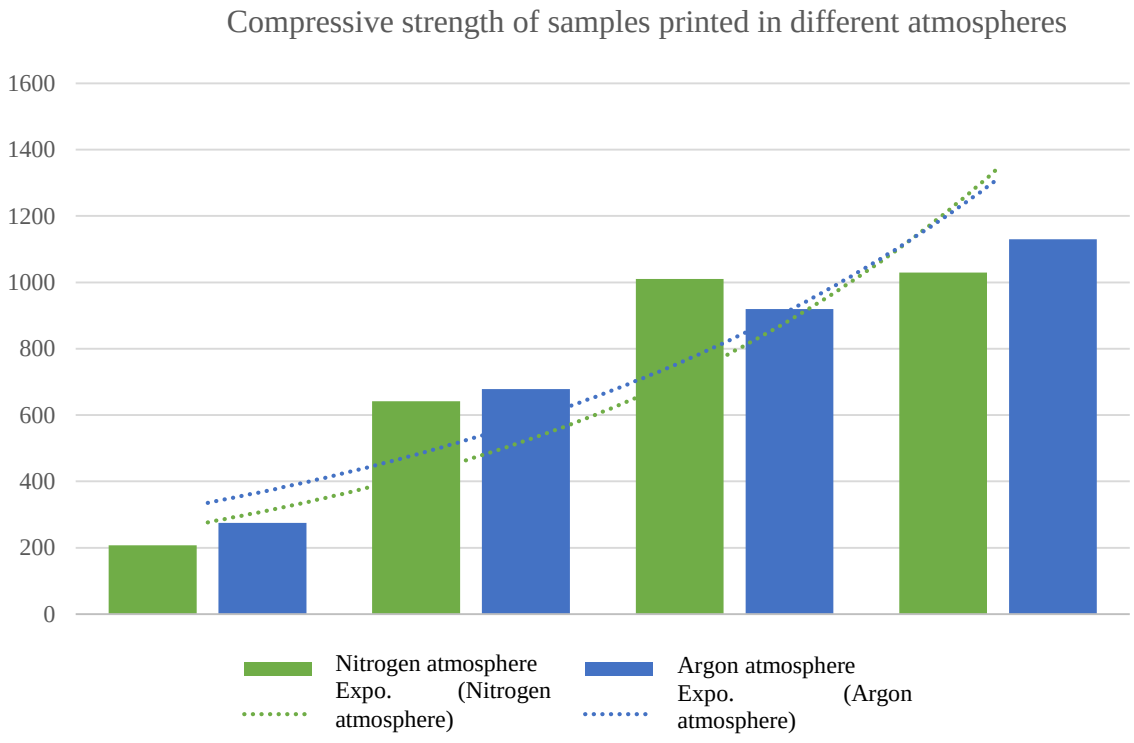
From the results outlined above in Figure 10, it follows that the carbon migrated from the WC grains to the binder in which the carbon filled the vacant places. As a result, CoCx phase formation and distortion of the crystal lattice occurred. Furthermore, this analysis confirmed that no intermediate CoNx phases were formed using nitrogen as a protective atmosphere. This is probably related to the rate at which the phase transformations occur and also to the fact that the carbon atoms have a lower atomic mass and thus diffuse at a lower energy preferably into the molten binder, which makes it impossible for the nitrogen to occupy the vacant places in the forming crystal lattice of the solidifying binder.

The samples were also subjected to micro-hardness measurement HV0.5, see Tab. 3 and compression strength testing, see Figure 11.

Input Energy Ev (J/mm^3)	**100**	**100**	**100**
Argon atmosphere	901±281	876± 281	827± 185
Nitrogen Atmosphere	1011± 91	891± 104	906± 116

Table 3. Micro hardness Vickers test HV0.5

Micro-hardness was measured on all the samples. Table 3 shows the comparison of the micro hardness measured on the binder on the samples that were printed at the same energy density Ev. The micro-hardness was approximately the same for all the test samples. The large variance in the measured values was probably due to the occurrence of pores in the sample structures. The pores meant that imprints could be created in places where the pores were hidden and measurement could be distorted, and affect the standard deviation of the measurement. A noticeable difference in standard deviations in samples printed in different atmospheres could be due to a higher proportion of micro-pores in the structure of samples printed in the atmosphere of argon, see Fig 4, or it could be due to more frequent hardness measurements near the hidden macro-pores.



	P (W)	V (mm/s)	Ev (J/mm^3)
Series of samples 1	120	100	100
Series of samples 2	200	166	100.4
Series of samples 3	280	233	100.1
Series of samples 4	360	300	100

Fig. 11 Compressive strength of printed samples at constant energy density Ev, but different scanning speeds and laser power.

The compressive strength was greatly influenced by the macro-pores, which were recorded both in the samples printed in the nitrogen atmosphere and in the argon atmosphere, see Figures 6-7. From the compression strength measurement, see Figure 11, it is seen that with increasing laser power and scanning speed, pores are eliminated in the structure of the printed samples and their compression strength increases. This is probably due to the fact that when a higher laser power is used, a higher temperature of the binder fluid is achieved. This means that the capillary-initiated binder may be molten for a longer period of time, so the wetted carbide grains will be pressed together for a longer time. *(Sarin et al., n.d.)* This is then reflected by reduced porosity in the printed samples.

3. CONCLUSION

The aim of this study was to assess the effect of nitrogen and argon atmospheres on the properties of printed samples of sintered carbide WC-Co. Based on metallographic analysis, X-ray phase composition analysis and mechanical properties testing, it is possible to state:

- Cracks, globular pores and non-globular pores were observed in the printed samples in both atmospheres before etching. These discontinuities occurred due to incorrect boundary conditions of the printing process, thermal stresses, wrong powder mixture and the action of residual moisture.

- Because both gases are inert to the binder and because of the speed at which the printing is performed, it was not possible to melt the powder and re-solidify it to produce intermediate phases of cobalt nitrides, as confirmed by X-ray analysis of the phase composition.
- By analysing the chemical composition near the pores, it was found that there was no loss of binder near them during the printing process. In addition, oxidation on the surface of the pores was proven. It can be concluded that most of the porosity detected by metallographic analysis was due to residual moisture, thermal stresses and the type of powder used in both atmospheres.
- The methods used to evaluate the mechanical properties of the printed samples in different atmospheres did not reveal any significant differences in their mechanical properties. The differences in the measured values were probably due to different binder distribution, carbide grains and porosity in the samples.

The results of the experiments show that it is possible to use nitrogen as a protective atmosphere when printing sintered carbides because it does not significantly affect the properties of the product. Its properties are similar to those obtained when printing in an argon atmosphere, and it is also cheaper than using an argon atmosphere.

Further experiments will focus on printing parts from different types of WC-Co powders, and other boundary conditions of the manufacturing process will also be tested, such as the thickness of the layer of the powder, different scanning speeds and laser powers.

ACKNOWLEDGMENTS

This study was carried out thanks to the mutual cooperation between the Institute for Nanomaterials, Advanced Technology and Innovation at the Technical University of Liberec, and Ceratizit. It was further supported by the SGS project 2016-36 “Analysis, development and modification of manufacturing technology in volume processing of advanced materials used in energy machinery, transport equipment and related engineering applications”.

REFERENCES

1. Venuvinod, P. and Ma, W. (2010). Rapid prototyping. Boston: Kluwer Academic
2. Uhlmann, E., Bergmann, A. and Gridin, W. (2015). Investigation on Additive Manufacturing of Tungsten Carbide-cobalt by Selective Laser Melting. Procedia CIRP, 35, pp.8-15.
3. Wang, X., Laoui, T., Bonse, J., Kruth, J., Lauwers, B. and Froyen, L. (2002). Direct Selective Laser Sintering of Hard Metal Powders: Experimental Study and Simulation. The International Journal of Advanced Manufacturing Technology, 19(5), pp.351-357.
4. Bricín, D., Špirit, Z. and Kříž, A. (2018). Metallographic Analysis of the Suitability of a WC-Co Powder Blend for Selective Laser Melting Technology. Materials Science Forum, 919, pp.3-9.
5. GU, D., SHEN, Y., DAI, P. and YANG, M. (2006). Microstructure and property of sub-micro WC-10 %Co particulate reinforced Cu matrix composites prepared by selective laser sintering. Transactions of Nonferrous Metals Society of China, 16(2), pp.357-362.
6. Kumar, S. (2009). Manufacturing of WC–Co moulds using SLS machine. Journal of Materials Processing Technology, 209(8), pp.3840-3848.
7. Pacurar, R. and Pacurar, A. (2016). Applications of the Selective Laser Melting Technology in the Industrial and Medical Fields. New Trends in 3D Printing.
8. Sutton, A., Kriewall, C., Leu, M. and Newkirk, J. (2016). Powder characterisation techniques and effects of powder characteristics on part properties in powder-bed fusion processes. Virtual and Physical Prototyping, 12(1), pp.3-29.

9. Sarin, V., Mari, D., Llanes, L. and Nebel, C. (n.d.). Comprehensive hard materials.
10. Palan, JA, (2015), Measuring of residual stress in relation to the technology of preparation, Master theisis. Pilsen: University of West Bohemia in Pilsen, Pilsen